Research in Astronomy and Astrophysics, 23:045010 (7pp), 2023 April https://doi.org/10.1088/1674-4527/acc14f

New Photometric Investigations of G-type Contact Binary TU Boo

Jing-jing Wang[1], Meng Guo[1], Lin-qiao Jiang[2], and Bin Zhang[3]
[1] China University of Petroleum–Beijing at Karamay, Karamay 834000, China; wangjingjing@cupk.edu.cn
[2] College of Mathematics and Physics, Leshan Normal University, Leshan 614000, China
[3] School of Physics and Electronic Science, Guizhou Normal University, Guiyang 550025, China
Received 2022 December 1; revised 2023 January 17; accepted 2023 February 20; published 2023 March 30

Abstract

Two sets of CCD photometric observations for contact binary TU Boo were obtained in 2020 and 2021. Different from its asymmetric light curves published from the literature, our BVR_cI_c-band curves show that the heights of maximum are almost equal. These distortions of light curves possibly indicate that the components were active in past 25 yr, but they were stable in the last two years. For total-eclipse binary TU Boo, due to some star-spots on the surface of the components, the physical structure obtained by many investigators are different. Therefore, the symmetric multi-color light curves in 2020, 2021 are important for understanding configuration and evolution of this system. By using the Wilson–Devinney program, it is confirmed that TU Boo is an A-type shallow-contact binary with the temperature difference of $\Delta T = 152$ K and fill-out of $f = 14.67\%$. In the $O-C$ diagram of orbital period analysis, a cyclic oscillation superimposed on a continuous decrease was determined. The long-term decreasing is often explained by the mass transfer from the more massive star to less massive one, this system will evolve into a deeper contact binary with time. The cyclic oscillations computed from much more CCD times of light minimum maybe result from the light-travel time effect via the presence of a third body. These characters of structure, evolution and ternary belong to typical A-type W UMa binaries with spectral G.

Key words: (stars:) binaries: eclipsing – stars: solar-type – stars: individual (TU Boo)

1. Introduction

Binnendijk (1970) defined A-subtype and W-subtype W UMa binaries on account of their characteristics of light curves. For A-type systems, the primary eclipse of the deeper minimum is caused by the occultation of the more massive component, while W-type ones are because of the less massive one. From these derived solutions, in A-type binaries, the temperature of the more massive component is the hotter one, and in W-type binaries, the less massive star is the hotter one. Actually, due to the common convective envelop (Lucy 1968) of contact binaries, the difference of the effective temperatures between two components are typically small. There are also some doubts about the evolution of the A- and W-subtype stars. Mochnacki & Whelan (1973) predicted that A-type W UMa binaries have low mass ratios, W-type binaries cannot evolve to A-type binaries of larger total mass (Gazeas & Niarchos 2006). Yakut & Eggleton (2005) suggested that rather than intrinsic/evolutionary trait, the dark spot coverage of the primary star plays a significant role in properties of W-type systems. The properties of the cool spots in W-type binaries are similar to those of sunspots generated by dynamos, which differ from those of the cool spots in A-type binaries (Kouzuma 2019). The temperature ratio possibly occurs reversal because of the spots on the component, while they found there is no correlation between the spotted/unspotted groups and the A/W types (Latković et al. 2021). Energy transfer in W-subtype systems caused over-luminosity of the secondary components, while that property in A-subtype is due to the secondary components that evolved from initial more massive stars (Zhang et al. 2020). Latković et al. (2021) present that spots influence the estimated temperature of both components to lead to the temperature ratio reversal, which might in turn result in type assignments. Thus, it is necessary to enrich much more physical properties of these A/W subtype binaries, and the G-type contact binary TU Boo is an interesting target.

Derived from the asymmetrical BV -band light curves (Niarchos et al. 1996), TU Boo (=GSC 2545 0864) was classified as an A-type W UMa contact binary with total eclipse. However, the authors found that its physical parameters are more common for a W-type system. On the basis of synthetic light-curve analysis, the fill-out factor was determined as 32%. Due to the ambiguity of two subtypes, the investigators had paid attention to this system. Lee et al. (2007) carried out BVR-band observations, which were with positive O'Connell effect. Their solutions suggest that TU Boo is an A-type system, and the fill-out factor of 17% is about 2 times smaller than 32% (Niarchos et al. 1996), it is unreasonable for the obvious variation of the degrees of contact within about 20 yr. Also, during the studies on the orbital period, they found that a quasi-sinusoidal term is superposed on a long-term decrease. The secular variation possibly comes from the mass transfer,

Table 1
Coordinates and Magnitudes of the Contact Binary TU Boo (V), the Comparison (C) and the Check Stars (Ch)

Stars	α_{2000}	δ_{2000}	$R_{\rm mag}$
TU Boo (V)	$14^{\rm h}04^{\rm m}58^{\rm s}.05$	$+30°00'01''.59$	12.09
GSC 2012-0831 (C)	$14^{\rm h}05^{\rm m}00^{\rm s}.31$	$+29°56'24''.04$	14.71
GSC 2012-0878 (Ch)	$14^{\rm h}04^{\rm m}59^{\rm s}.00$	$+29°52'34''.07$	11.39

and the periodic changes from the light-time effect or magnetic activity. However, Coughlin (2010) analyzed their *UBVRI*-band light curves to re-classify that TU Boo as a near-contact or barely semi-detached system with three cool spots, which could explain the anomalies presented by Niarchos et al. (1996). If the configuration was truly accurate, this binary would be a keystone in understanding A-type evolving to W-type. From the analysis of $O-C$, the most noticeable abrupt change around JD 2452000 was found, Coughlin (2010) proposed that this phenomenon is most likely due to the rapid mass transfers between the two components.

In this paper, we present two sets of CCD photometric observations for TU Boo in 2020 and 2021, the total-eclipse and symmetric curves are helpful for obtaining the photometric solutions. Thanks to the accumulation of CCD minimum times from the literature during the past 15 yr, the orbital period is re-analyzed. The evolution, configuration, and the ternary nature are discussed in detail.

2. Observations

The complete four-color photometric observations of G-type contact binary TU Boo were carried on 2020 April 27 and 2021 April 3 separately, with the DZ936N 2048×2048 CCD camera attached to the 60 cm telescope at XingLong Station (XLS) of National Astronomical Observatories of the Chinese Academy of Sciences. The integration times was 60 s for the *B* band, 40 s for the *V* band, 30 s for the *R* band, and 20 s for the *I* band. The variable (V) of TU Boo, the comparison star (C), and the check star (CH) are close to each other, their coordinates and magnitudes are listed in Table 1. The PHOT task in the IRAF aperture photometry package was used to reduce the observed images, including a flat field correction process (Kallrath & Milone 1999). The mean photometric errors for individual observations are 0.006 mag in the *BI*-band, and 0.005 mag in the *VR*-band, respectively.

All two sets of observations were obtained in one night, these light curves along with their differential magnitudes (Δm) and Heliocentric Julian Date (HJD) are displayed in Figure 1. The light curves are nearly symmetric, and belong to EW-type. The magnitude differences of the comparison star (C) minus that of the check star (CH) are shown in the lower part of Figure 1. The distortions and O'Connell effect (Niarchos et al. 1996; Lee et al. 2007; Coughlin 2010) have been variable in the past, therefore we look forward to much more variations to investigation on the magnetic activities. However, the upper points of Figure 1 display the height of light curves in 2020 and 2021 are nearly the same and symmetric with total eclipse, maybe the activities on the surface of the components are weak. These observations are also helpful for us to explore more reliable photometric solutions, and analyze the evolution structure.

3. Photometric Solutions with the Wilson–Devinney Program

Based on the *BV*-band light curves, Niarchos et al. (1996) searched the lowest weighted squares of the residuals for different mass ratio q, and proposed that TU Boo is an A-type contact binary with $q=0.498$. The effective temperature of the secondary component is 5805 K, slightly higher than the primary component 5800 K. According to the definitions of A-subtype and W-subtype (Binnendijk 1970), although the difference of temperature is very small, the primary one should be the hotter stars for A-type contact binaries. Lee et al. (2007) also made the same way to reveal that it is an typical A-type system with $q=0.508$, $T_1=5800$ K, $T_2=5737$ K. However, via the fitting of *UBVRI*-band light curves, Coughlin (2010) suggested that TU Boo is a near-contact or barely semi-detached system with $q=0.481$, $T_1=5821$ K, $T_2=5691$ K. In these investigations, their asymmetric light curves were fitting with the different spot. Did the spot make influence on the structure? It is unknown. The complete multi-color observations in 2020 and 2021 are symmetric and important to acquire suitable solutions. To investigate the magnetic activities and structure of this binary, our light curves in 2020 and 2021 were analyzed with version 2013 Wilson–Devinney program (Wilson & Devinney 1971; Wilson 1979, 1990; Van Hamme & Wilson 2007; Wilson 2008).

According to LAMOST spectral analysis, the effective temperature was $T=5796$ K in 2014, $T=5695$ K in 2016, $T=5803$ K in 2017 (Qian et al. 2020), then we took the average temperature $T_1=5764$ K for the primary star (star eclipsed at primary light minimum). In addition, considering the convective atmospheres of the components, the same values of the gravity-darkening coefficients and the bolometric albedo, i.e., $g_1=g_2=0.32$ (Lucy 1967) and $A_1=A_2=0.5$ (Ruciński 1969) were fixed. The mass ratio $q=M_2/M_1$, the orbital inclination i, the mean temperature of the secondary component T_2, the dimensionless potentials of each component Ω_1, Ω_2, and the monochromatic luminosity of primary component for every band L_{1B}, L_{1V}, L_{1R}, L_{1I} were adjustable.

From Figure 1, the light curves in 2020 are nearly the same as that in 2021. Due to the conditions of the weather, the observations in 2020 show better. We first analyze the complete *BVRI*-band curves in 2020. Later, to check our photometric solutions, these converged parameters were used

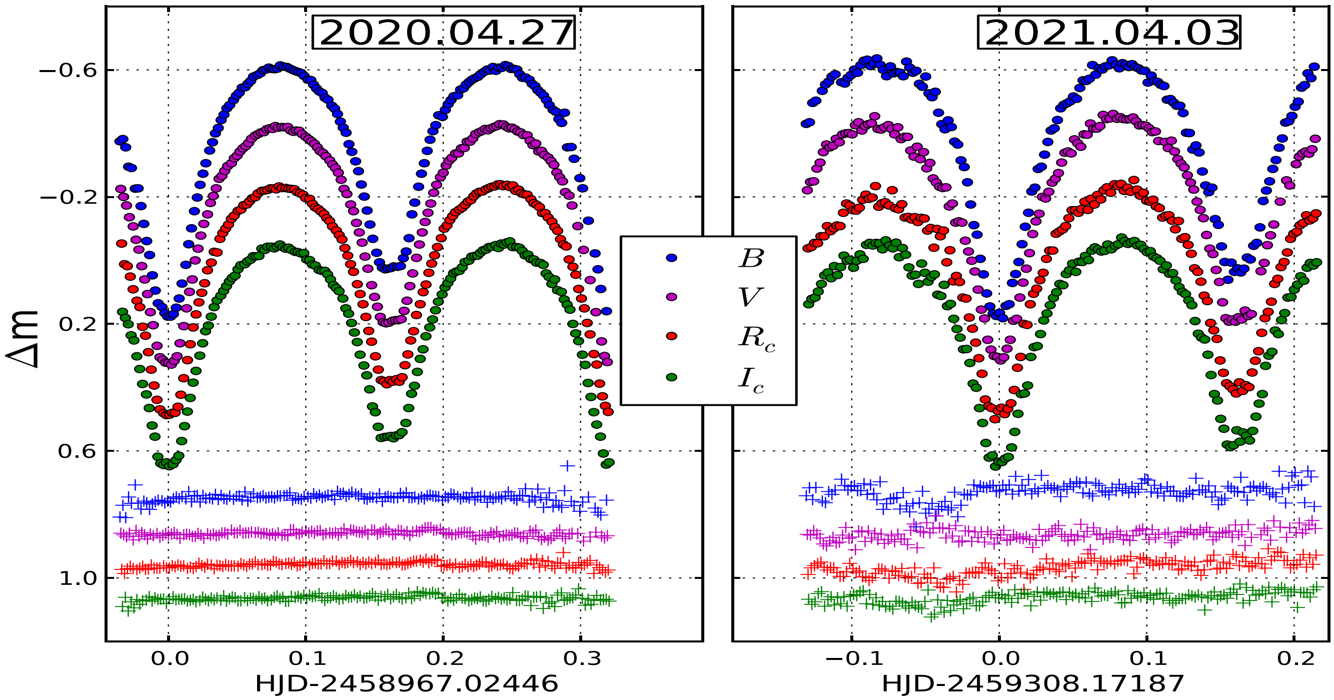

Figure 1. (Top) *BVRI*-band observations of TU Boo in 2020 and 2021, with the 60 cm telescope at XingLong Station. (Bottom) The plus refers to *BVRI*-band magnitudes of the comparison star minus the check star (C-Ch). The HJD2458967.02446 and HJD 2 459 308.171 87 are the times of primary light minimum, corresponding to the horizontal coordinate 0.0.

Table 2
Photometric Solutions for TU Boo

Parameters	Photometric Elements	Errors	Parameters	Photometric Elements	Errors
$g_1 = g_2$	0.32	Assumed	$L_1/(L_1 + L_2)$ (B)	0.6907	±0.0017
$A_1 = A_2$	0.5	Assumed	$L_1/(L_1 + L_2)$ (V)	0.6821	±0.0015
LD	−3	Assumed	$L_1/(L_1 + L_2)$ (R)	0.6775	±0.0014
$x_{1\text{bol}}, y_{1\text{bol}}$	0.541,0.172	Assumed	$L_1/(L_1 + L_2)$ (I)	0.6742	±0.0014
$x_{2\text{bol}}, y_{2\text{bol}}$	0.638,0.163	Assumed	r_1(pole)	0.4226	±0.0010
T_1	5764 K	Assumed	r_1(side)	0.4506	±0.0013
T_2	5612 K	±5 K	r_1(back)	0.4815	±0.0018
q (M_2/M_1)	0.495	±0.006	r_2(pole)	0.2838	±0.0011
Ω_{in}	2.8660		r_2(side)	0.2943	±0.0013
Ω_{out}	2.5702		r_2(back)	0.3188	±0.0019
$\Omega_1 = \Omega_2$	2.8226	±0.0054	f	14.67%	±1.81%
i	88.794	±0.274	$\Sigma\omega(O - C)^2$	0.0000413	

to make the fitting curves in 2021. If the fitting curves are consistent with the *BVRI*-band observation, the derived results are reasonable and credible.

Though there is no mass ratio from spectroscopic observations, the photometric mass ratios are in good agreement with the spectroscopic ones for almost all of the totally eclipsing systems (Pribulla et al. 2003; Terrell & Wilson 2005; Li et al. 2021). In the past three studies (Niarchos et al. 1996; Lee et al. 2007; Coughlin 2010), the mass ratios for TU Boo are $q = 0.498$, $q = 0.508$, and $q = 0.481$, close to each other. Thus, we applied mass ratio $q = 0.500$ as an adjustable to perform the Differential Corrections program (DC). As shown in Table 2, the parameters suggest that TU Boo is an A-type shallow-contact binary without spot. The theoretical light curves were displayed in Figure 2. Compared with the solutions, the structure of this binary obtained by us are nearly the same as that by Lee et al. (2007), whose investigations suggest that there are some spots on the surface of the component. Maybe

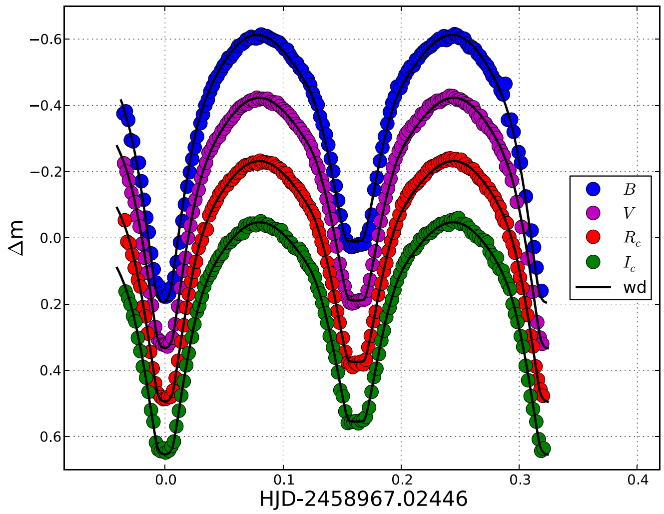

Figure 2. Theoretical light curves for TU Boo in 2020.

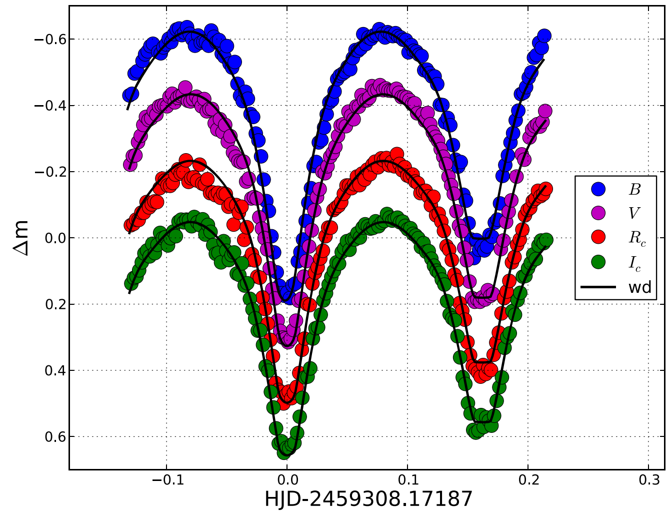

Figure 3. Theoretical light curves for TU Boo in 2021.

the magnetic activities are variable, we simply were lucky to observed this system in the weak activities. In order to check our derived parameters, they were used to produce fitting curves in 2021, by use of Light Curve program (LC) in WD, where curves were plotted in Figure 3. It is noted that the theoretical curves are tally with observations, what suggest our solutions are reliable. The geometrical structure at phases 0.0, 0.25, 0.50 are 0.75 as shown in Figure 4.

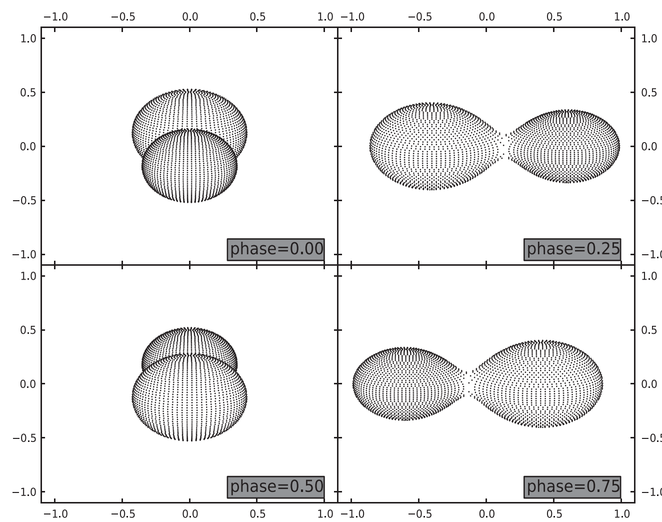

Figure 4. Geometric configurations of TU Boo at phase 0.00, 0.25, 0.50, 0.75.

4. Variations of the $O-C$ Diagram

Orbital period changes of TU Boo have been studies by several authors (Szafraniec 1952; Niarchos et al. 1996; Lee et al. 2007; Coughlin 2008, 2010), Niarchos et al. (1996) found a period shortening of 0.413 s around JD 2445425. Lee et al. (2007) analyzed the resulting $O-C$ diagram to reveal that the orbital period has varied in a quasi-sinusoidal way superposed on a long-term period decrease. Meanwhile, Coughlin (2008), Coughlin (2010) thought that there is a noticeable abrupt change around JD 2452000, it is possibly due to rapid, large-scale mass transfer between the components. In these investigations, the vast majority of times are the photographic and the visual ones, CCD eclipse times were less over a span of 13 yr. Since 2007, this binary has been observed further for 15 yr by some telescopes equipped with CCD. Thus, we attempt to re-analyze the orbital period to explore the evolutional state of TU Boo. Most of the timings come from the database published by Kreiner et al. (2001), Lee et al. (2007), Coughlin (2008), Coughlin (2010), a lot of visual and photometric timings have also been published with no errors, and were fixed as ±0.005 days. The other available timings complied from the newly literature and our CCD measurements, are listed in Table 3. In case of CCD observations without error, a value of ±0.0005 days was assumed.

Based on the ephemeris equation (Lee et al. 2007),

$$\text{Min. } I \text{ (HJD)} = 2445055.5666 + 0^{\mathrm{d}}.324284504 \times E, \quad (1)$$

we calculated the $(O-C)_1$ values, which were plotted in the upper panel of Figure 5. The green pluses refer to the photographic and visual times of light minimum, the blue circles represent photoelectric and CCD ones. To find the secular variations of the $(O-C)_1$, the photographic timings HJD24609.3320, HJD24609.3370, HJD24614.3400, HJD24615.3400, HJD24616.3100, HJD24621.4900, HJD24650.3400, HJD29732.3500, and HJD30088.4500 with red circles were removed because of larger deviation. By using a least-square fitting method, a parabola plus cyclic term was applied to fit all of these data, the new ephemeris was obtained as follows (Irwin 1952;

Table 3
Other CCD Timings of Light Minimum for TU Boo

HJD	Errors	Ref.	HJD	Errors	Ref.	HJD	Errors	Ref.
2451679.4028	0.0015	Agerer & Hubscher (2002)	2454941.5280	0.0008	Hubscher et al. (2010)	2457093.4798	0.0000	Brát et al. (2007)
2452863.3660	0.0060	Diethelm (2004)	2454961.7925	0.0003	Hubscher et al. (2010)	2457099.4790	0.0000	Brát et al. (2007)
2453091.8161		$O-C$ gateway	2455259.8104	0.0001	Samolyk (2011a)	2457130.2814		$O-C$ gateway
2453115.6518		$O-C$ gateway	2455279.7547	0.0001	Samolyk (2011a)	2457466.4003	0.0006	IBVS 6196
2453175.6439		$O-C$ gateway	2455342.3398	0.0001	Samolyk (2011a)	2457466.5636	0.0010	IBVS 6196
2453186.6688		$O-C$ gateway	2455592.5267	0.0000	Hubscher & Lehmann (2012)	2457840.6211	0.0000	$O-C$ gateway
2453374.5920	0.0030	Locher (2005)	2455602.5803	0.0000	Hubscher & Lehmann (2012)	2457855.3814	0.0000	IBVS 6244
2453574.6733		$O-C$ gateway	2455629.6569	0.0004	Samolyk (2011b)	2457855.5422	0.0027	IBVS 6244
2453765.5145	0.0003	Hubscher (2006)	2455637.9264	0.0002	Diethelm (2011)	2457874.3519	0.0003	IBVS 6244
2453834.7499		$O-C$ gateway	2455647.8175	0.0004	Samolyk (2011b)	2457874.5135	0.0002	IBVS 6244
2453867.5030	0.0003	Hubscher (2007)	2455661.4382	0.0004	Hubscher et al. (2012)	2458132.9680		$O-C$ gateway
2454192.7576		$O-C$ gateway	2455661.6007	0.0010	Hubscher et al. (2012)	2458227.4998		$O-C$ gateway
2454199.4045	0.0003	Hubscher (2014)	2455690.7841	0.0002	Diethelm (2011)	2458231.7121		$O-C$ gateway
2454205.4042	0.0003	Brát et al. (2007)	2455924.5934	0.0005	Banfi et al. (2012)	2458486.9244		$O-C$ gateway
2454211.4025	0.0002	Dogru et al. (2007)	2455982.4782	0.0001	Samolyk (2013a)	2458498.9219		$O-C$ gateway
2454219.6723		$O-C$ gateway	2455982.6412	0.0001	Samolyk (2013a)	2458533.9460		$O-C$ gateway
2454224.3744	0.0001	Hubscher et al. (2009)	2456003.8809	0.0002	Diethelm (2012)	2458573.8320		$O-C$ gateway
2454235.7227		$O-C$ gateway	2456069.5493	0.0012	Hubscher & Lehmann (2012)	2458924.8680		$O-C$ gateway
2454520.7686	0.0001	Samolyk (2008a)	2456075.7098	0.0003	Diethelm (2012)	2458956.6477		$O-C$ gateway
2454556.7644	0.0001	Samolyk (2008b)	2456336.9210	0.0002	Samolyk (2013b)	2459215.2648		$O-C$ gateway
2454562.7650	0.0002	Samolyk (2008b)	2456369.8361	0.0001	Samolyk (2013b)	2459244.2884		$O-C$ gateway
2454563.7380	0.0003	Samolyk (2008b)	2456411.8305	0.0006	Samolyk (2013b)	2459300.0653		$O-C$ gateway
2454583.6791	0.0002	Samolyk (2008b)	2456456.4197	0.0001	Hoňková et al. (2013)	2459300.2276		$O-C$ gateway
2454871.8062	0.0001	Samolyk (2009)	2456720.8736	0.0001	Samolyk (2014)	2458967.18640	0.0003	Ours
2454895.8029	0.0002	Nelson (2010)	2456795.6194	0.0001	Samolyk (2014)	2458967.02446	0.0001	Ours
2454939.7427	0.0002	Samolyk (2010)	2457082.7738		$O-C$ gateway	2459308.17187	0.0002	Ours
2454941.3650	0.0010	Hubscher et al. (2010)	2457084.8811		$O-C$ gateway	2459308.33384	0.0003	Ours

Sterken 2005),

$$\begin{aligned} \text{Min. } I = & \ 2445055.59166(\pm 0.00064) \\ & + 0\overset{\text{d}}{.}32428469(\pm 0.000000016) \times E \\ & - 2.88 \times 10^{-11}(\pm 0.38) \times E^2, \\ & + 0.01896(\pm 0.00059)\sin(0\overset{\circ}{.}05760(\pm 0.00015) \\ & \times E - 74°57(\pm 2°07)) \end{aligned} \quad (2)$$

the downward parabolic change indicates that the period is continuously decreasing, which the long-term period decreases at a rate of $dP/dt = -6.49 \times 10^{-8}$ days yr^{-1}. In the middle panel of Figure 5, the red solid line represents the oscillation with an amplitude of 0.018 96 days and a period of 55.49 yr. The corresponding residuals from Equation (2) are displayed in the lower panel of Figure 5.

5. Discussion and Conclusion

The published light curves (Niarchos et al. 1996; Lee et al. 2007; Coughlin 2008, 2010) of G-type contact binary TU Boo show positive O'Connell effect and obvious variation. These properties indicate that there are possible magnetic activities on the surface of the components. In previous investigations, the authors have employed some spots to model their asymmetry observations, the star-spots and structure of this system are listed in Table 4. Specially, Niarchos et al. (1996) introduced a cool spot on the larger component and a hot spot on the other one. Although they present that TU Boo is an A-type W UMa binaries, the temperature of the secondary component are slightly hotter than that of the primary one. Lee et al. (2007) invoked a cool spot and a hot spot on the secondary to confirm TU Boo as A-type system with $\Delta T = T_1 - T_2 = 63$ K. Coughlin (2010) allowed for two cool spots on primary and one cool spots on secondary, this binary were determined as a near-contact or barely semi-detached system. The configuration and evolution state are still indistinct.

In this paper, two sets of high-precision *BVRI*-band light curves for TU Boo observed in 2020 and 2021 respectively. As displayed in Figure 1, the symmetric light curves are first obtained, and significant for understanding the structure and

Table 4
Derived Starspots, Temperature, Structure for TU Boo in Different Time

Time of Observation	Primary		Secondary		Structure	Ref.
	Starspot	T_1	Starspot	T_2		
1982	a cool spot	5800 K	a hot spot	5805 K	A-type W UMa	Niarchos et al. (1996)
2007	None	5800 K	a cool spot a hot spot	5737 K	A-type W UMa	Lee et al. (2007)
2006	two cool spots	5821 K	a cool spot	5691 K	near-contact or semi-detached	Coughlin (2010)
2020 and 2021	None	5764 K	None	5612 K	A-type W UMa	Our present work

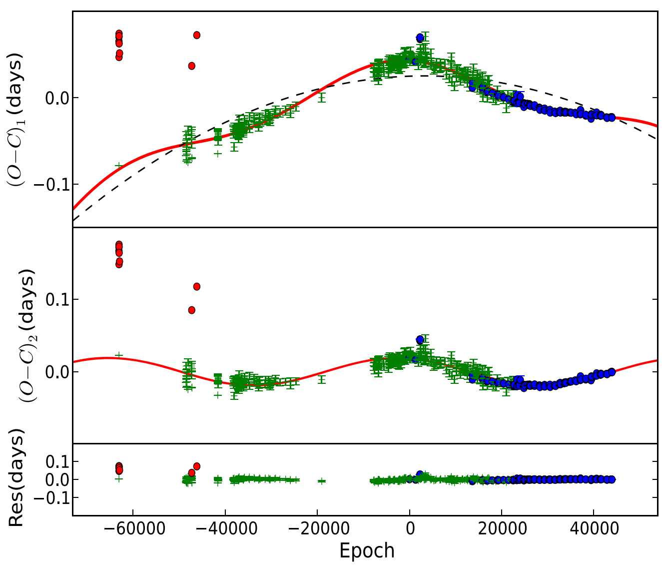

Figure 5. The $O-C$ diagram for TU Boo. Blue dots represent CCD times of light minimum, the green dots represent visual and photographic ones, the red dots represent the removed times with larger deviation. (Top) The solid line refers to a combination of the quadratic trend and a cyclic period change. (Middle) The solid line refers to the cyclic change. (Bottom) The residuals are with respect to Equation (2).

activities. These symmetric observations in 2020 and 2021 indicate weak photospheric activity on the surface of two components. By use of the 2013 version of W-D program, the final solutions confirm that TU Boo is a typical A-type contact binary with total eclipsing, and the temperature difference of $\Delta T = T_1 - T_2 = 152$ K, where both components share a common convective envelope without strong spot activities. The fill-out factor of $f = 14.67\%$ suggest TU Boo is a shallow contact binary.

Liao et al. (2021) suggest most of G-type shallow contact binaries are undergoing a long-term and periodic orbital period changes, and there are more systems show long-term decrease. In the $O-C$ diagram of Figure 5, the long-term decreasing superposed the cyclic oscillation were found for TU Boo. The orbital period of TU Boo is decreasing at a rate of $dP/dt = -6.49 \times 10^{-8}$ days yr^{-1}, the cyclic variations of $A_3 = 0.01896$ days and $P_3 = 55.49$ yr are close to that proposed by Lee et al. (2007). The secular decrease of orbital period maybe come from mass transfer from the more massive star to the less massive one. Kouzuma (2019) investigated the statistical properties of star-spots in eclipsing binaries stars, and inferred that mass transfer is an important origin of the hot-spots in A-type binaries. In Table 4, the hot spots found in 1982 and 2007 are possible. With the secular decrease of period, the orbital of this system will shrink, and the degree of over-contact become higher. Therefore, this system will evolve into a deeper contact binary. Compared with possible sinusoidal change (Lee et al. 2007), the cyclic oscillations in $O-C$ diagram of much more CCD times were usually explained by the light-travel time effect via the presence of a third body (Liao & Qian 2010; Qian et al. 2011, 2012; Zhu et al. 2013a, 2013b; Qian et al. 2015). The properties are similar to some A-type total-eclipse binaries, such as AU Tau (Xiang et al. 2015a; Tvardovskyi et al. 2018), V508 Oph (Xiang et al. 2015b), EQ Tau (Li et al. 2014).

To investigate the evolution state of the components, by using the 3D correlation equations on physical parameters (i.e., mass, radius and luminosity) of contact binaries supplied by Gazeas (2009), the absolute dimensions are estimated as $M_1 = 1.08(\pm 0.05)M_\odot$, $M_2 = 0.53(\pm 0.03)M_\odot$, $R_1 = 1.05(\pm 0.05)R_\odot$, $R_2 = 0.78(\pm 0.04)R_\odot$, $L_1 = 1.05(\pm 0.05)L_\odot$, $L_2 = 0.57(\pm 0.03)L_\odot$. There parameters are good agreement with evolutional scenario, in which contact binaries has achieved equilibrium after mass ratio reversal (Stepien 2006). With regards to the structure that the components fill their Roche lobes, the evolution of these stars in system are possibly different from the single main sequence (MS) stars. The primary components are close to MS stars, the secondary components are brighter and larger than MS stars of the same mass. Latković et al. (2021) made statistics of 700 individually studied W UMa binaries to reveal their HR diagram, mass–radius and mass–luminosity relation. They concluded that primary components occupy the region of unevolved low-mass single stars, while the secondaries are systematically over-sized and over-luminous. The characteristic is an expected consequence of the energy exchange through the common envelope. Therefore, the secondary component is treated as the key to the acknowledge of W UMa type binaries

(Yakut & Eggleton 2005; Yildiz & Doğan 2013). In order to detect magnetic activities and evolution, it is necessary to obtain many high-precision photometric and RV curves of TU Boo.

Acknowledgments

The CCD photometric observations of TU Boo were obtained with the 60 cm telescope at Xinglong observational station of National Astronomical Observatories, Chinese Academy of Sciences. This work is sponsored by Natural Science Foundation of Xinjiang Uygur Autonomous Region (No. 2022DO1A164), the Joint Research Found (No. U1831109) in Astronomy under cooperative agreement between the National Natural Science Foundation of China (NSFC) and Chinese Academy of Sciences (CAS), and the Natural Science Foundation of Shandong Province (No. ZR2020QA048).

ORCID iDs

Jing-jing Wang https://orcid.org/0000-0002-9947-9263

References

Agerer, F., & Hubscher, J. 2002, IBVS, 5296, 1
Banfi, M., Aceti, P., Arena, C., et al. 2012, IBVS, 6033, 1
Binnendijk, L. 1970, VA, 12, 217
Brát, L., Zejda, M., & Svoboda, P. 2007, OEJV, 74, 1
Coughlin, J. L. 2010, arXiv:1004.1395
Coughlin, J. L., Dale, H. A., III., & Williamon, R. M. 2008, AJ, 136, 1089
Diethelm, R. 2004, IBVS, 5543, 1
Diethelm, R. 2011, IBVS, 5992, 1
Diethelm, R. 2012, IBVS, 6029, 1
Dogru, S. S., Dogru, D., & Donmez, A. 2007, IBVS, 5795, 1
Gazeas, K. D. 2009, CoAst, 159, 129
Gazeas, K. D., & Niarchos, P. G. 2006, MNRAS, 370, 29
Hoňková, K., Juryšek, J., & Lehký, M. 2013, OEJV, 160, 1
Hubscher, J. 2007, IBVS, 5802, 1
Hubscher, J. 2014, IBVS, 6118, 1
Hubscher, J., & Lehmann, P. B. 2012, IBVS, 6026, 1
Hubscher, J., Lehmann, P. B., & Walter, F. 2012, IBVS, 6010, 1
Hubscher, J., Paschke, A., & Walter, F. 2006, IBVS, 5731, 1
Hubscher, J., Steinbach, H. M., & Walter, F. 2009, IBVS, 5874, 1
Hubscher, J., Lehmann, P. B., Monniger, G., Steinbach, H. M., & Walter, F. 2010, IBVS, 5918, 1
Irwin, J. B. 1952, ApJ, 116, 211
Kallrath, J., & Milone, E. F. 1999, Eclipsing Binary Stars: Modeling and Analysis (New York: Springer), 43
Kouzuma, S. 2019, PASJ, 71, 21
Kreiner, J. M., Kim, C. H., & Nha, I. S. 2001, An Atlas of O-C Diagrams of Eclipsing Binary Stars (Cracow: Wydawnictwo Naukowe Akademii Pedagogicznej)
Latković, O., Čeki, A., & Lazarević, S. 2021, ApJS, 254, 10
Lee, J. W., Kim, H. I., & Kim, S. L. 2007, PASP, 119, 1099
Li, K., Qian, S. B., Hu, S. M., & He, J. J. 2014, AJ, 147, 98
Li, K., Xia, Q. Q., Kim, C. H., et al. 2021, AJ, 162, 13
Liao, W. P., Li, L. J., Zhou, X., et al. 2021, RAA, 21, 41
Liao, W. P., & Qian, S. B. 2010, MNRAS, 405, 1930
Locher, K. 2005, OEJV, 3, 1
Lucy, L. B. 1967, ZA, 65, 89
Lucy, L. B. 1968, ApJ, 151, 1123
Mochnacki, S. W., & Whelan, J. A. J. 1973, A&A, 25, 249
Nelson, R. H. 2010, IBVS, 5929, 1
Niarchos, P. G., Hoffmann, M., & Duerbeck, H. W. 1996, A&AS, 117, 105
Pribulla, T., Kreiner, J. M., & Tremko, J. 2003, CoSka, 33, 38
Qian, S.-B., Han, Z.-T., Fernández Lajús, T., et al. 2015, ApJS, 221, 17
Qian, S.-B., Liu, L., Zhu, L. Y., et al. 2012, MNRAS, 422, 24
Qian, S.-B., Liu, L., Liao, W.-P., et al. 2011, MNRAS, 414, 16
Qian, S. B., Zhu, L. Y., Liu, L., et al. 2020, RAA, 20, 163
Ruciński, S. M. 1969, AcA, 19, 245
Samolyk, G. 2008a, JAVSO, 36, 171
Samolyk, G. 2008b, JAVSO, 36, 186
Samolyk, G. 2009, JAVSO, 37, 44
Samolyk, G. 2010, JAVSO, 38, 85
Samolyk, G. 2011a, JAVSO, 39, 94
Samolyk, G. 2011b, JAVSO, 39, 177
Samolyk, G. 2013a, JAVSO, 41, 122
Samolyk, G. 2013b, JAVSO, 41, 328
Samolyk, G. 2014, JAVSO, 42, 426
Stepien, K. 2006, AcA, 56, 199
Sterken, C. 2005, ASPC, 335, 181
Szafraniec, R. 1952, AcA, 2, 86
Terrell, D., & Wilson, R. E. 2005, Ap&SS, 296, 221
Tvardovskyi, D. E., Marsakova, V. I., Andronov, I. L., & Shakun, L. S. 2018, OAP, 31, 103
Van Hamme, W., & Wilson, R. E. 2007, ApJ, 661, 1129
Wilson, R. E. 1979, ApJ, 234, 1054
Wilson, R. E. 1990, ApJ, 356, 613
Wilson, R. E. 2008, ApJ, 672, 575
Wilson, R. E., & Devinney, E. J. 1971, ApJ, 166, 605
Xiang, F. Y., Xiao, T. Y., & Yu, Y. X. 2015a, AJ, 150, 25
Xiang, F. Y., Yu, Y. X., & Xiao, T. Y. 2015b, AJ, 149, 62
Yakut, K., & Eggleton, P. P. 2005, ApJ, 629, 1055
Yildiz, M., & Doğan, T. 2013, MNRAS, 430, 2029
Zhang, X. D., Qian, S. B., & Liao, W. P. 2020, MNRAS, 492, 4112
Zhu, L. Y., Qian, S. B., Liu, N. P., Liu, L., & Jiang, L. Q. 2013a, AJ, 145, 39
Zhu, L. Y., Qian, S. B., Zhou, X., et al. 2013b, AJ, 146, 28